Stickiness and cantori

1997 J. Phys. A: Math. Gen. 30 8167

(http://iopscience.iop.org/0305-4470/30/23/016)

J. Phys. A: Math. Gen. **30** (1997) 8167–8186. Printed in the UK PII: S0305-4470(97)84671-9

Stickiness and cantori

C Efthymiopoulos†‡, G Contopoulos†, N Voglis† and R Dvorak‡

† Department of Astronomy, University of Athens, Panepistimiopolis, 157 84-Athens, Greece
‡ Institut für Astronomie, Universitat Wien, Türkenschanzstrasse 17, A-1180, Wien, Austria

Received 2 June 1997, in final form 5 August 1997

Abstract. We study the phenomenon of stickiness in the standard map. The sticky regions are limited by cantori. Most important among them are the cantori with noble rotation numbers, that are approached by periodic orbits corresponding to the successive truncations of the noble numbers. The size of an island of stability depends on the last KAM torus. As the perturbation increases, the size of the KAM curves increases. But the outer KAM curves are gradually destroyed and in general the island decreases. Higher-order noble tori inside the outermost KAM torus are also destroyed and when the outermost KAM torus becomes a cantorus, the size of an island decreases abruptly. Then we study the crossing of the cantori by asymptotic curves of periodic orbits just inside the cantorus. We give an exact numerical example of this crossing (non-schematic) and we find how the asymptotic curves, after staying for a long time near the cantorus, finally extend to large distances outwards. Finally, we find the relation between the forms of the sticky region and asymptotic curves.

1. Introduction

The phenomenon of stickiness was observed (Contopoulos 1971) while an effort was made to numerically find the 'last KAM curve' around an island of stability in a Hamiltonian system of 2 degrees of freedom. While calculating invariant curves further and further away from the centre of an island, we found an orbit that looked ordered for a long time, but then its consequents diffused into the large chaotic sea outside the island. Several tests established that this was real, and not due to the limited accuracy of the calculations. The most convincing test was the inversion of the orbit after reaching the chaotic sea. The inverse orbit, after some iterations, was trapped for a long time around the island.

This phenomenon, named 'stickiness' by Shirts and Reinhardt (1982), was observed later by several authors. It is now obvious that stickiness is due to the existence of one or more cantori with small holes surrounding the island of stability.

Cantori are the 'remnants' of KAM tori when these tori are destroyed by increasing the nonlinearity parameter. They are infinite sets of points that are invariant but nowhere dense. In fact they are Cantor sets of zero measure. Cantori were found theoretically by Aubry (1978) and independently by Percival (1979), who gave them their name.

A cantorus forms a countable infinity of gaps. Although it contains uncountably many points, these have not only zero measure, but also zero Hausdorff dimension (see Meiss 1992 for further discussion and references). In this respect they are like periodic orbits of infinite period.

Furthermore, cantori can be approached by high-order periodic orbits. In fact both tori and cantori are characterized by irrational rotation numbers, that can be approximated by

0305-4470/97/238167+20$19.50

rationals. The best method to approximate these irrationals is by the successive truncations of their continued fraction representations.

Greene (1979) conjectured that the last KAM tori are those with 'noble' rotation numbers, i.e. continued fractions

$$a = [a_1, a_2, \ldots] \equiv \frac{1}{a_1 + \frac{1}{a_2 + \cdots}} \tag{1}$$

(where a_i are integers) that have $a_i = 1$ for all i above a certain order N. According to Greene these tori are destroyed when all the periodic orbits with rotation numbers equal to high-order truncations of a noble number become unstable.

Greene's conjectures have been verified in many cases up to now. An implementation of Greene's approach was given by Contopoulos *et al* (1987) in finding the value of the nonlinearity parameter, K_c, at which the last KAM torus is destroyed. This was done by extrapolating the values of K at which nearby periodic orbits become unstable. We must stress that the transition to instability for families of periodic orbits (with rotation numbers truncations of the noble number) occurs for values of K *larger* than K_c and these values tend to K_c as the rotation numbers of the corresponding periodic orbits tend to the noble number. Thus the critical value K_c is the *minimum* of the transition values of K for periodic oribts approaching the critical torus.

The simplest noble number is the golden mean

$$a = [1, 1, 1, \ldots] = \tfrac{1}{2}(\sqrt{5} - 1) \tag{2}$$

and according to Greene it is the last to be destroyed, as K increases. However, in some cases other noble tori may be more robust; in fact the local structure of phase space around each noble torus may be more important (Contopoulos *et al* 1987) in defining a local critical value for the destruction of a noble torus.

After a noble torus becomes a cantorus other orbits can cross its gaps and a diffusion phenomenon appears. This diffusion has been studied by many authors, for example, Bensimon and Kadanoff (1984) and MacKay *et al* (1984) developed a theory of diffusion through cantori for a value of the nonlinearity parameter K slightly above the critical value K_c. However, for even larger nonlinearity K the gaps of the cantorus increase rapidly with K and the diffusion through them is quite fast.

The theory of cantori and stickiness has still many unsolved problems (see, e.g. the review of Meiss 1992). It has been stated, correctly, by some people, that the most basic approach to these problems is by studying the forms of the asymptotic curves of the unstable periodic orbits in the sticky region. In fact diffusion through cantori does not occur in a probabilistic way, as assumed by some models (Markov models, Meiss 1992). It occurs along particular lobes, formed by the asymptotic curves of the unstable periodic orbits, that pass through the gaps of cantori. Thus diffusion affects the whole set of points inside a lobe, and individual points are not affected completely stochastically. However, the problem of the crossing of the cantori by lobes has only been considered schematically up to now (Meiss 1992).

A systematic study of the real forms of the lobes in certain simple maps is needed. At the same time we need the forms of the cantori. A comparison of the two will show how the lobes cross the gaps to generate diffusion.

In a recent paper (Contopoulos *et al* 1997) we studied the diffusion time in various parts of a sticky region. The stickiness time seems to depend in general exponentially on the distance from the last KAM curve around an island. However, very close to the last KAM curve the stickiness time seems to be superexponential. It is important to explain these phenomena in terms of the crossing of the cantori by lobes.

Another phenomenon found in that paper is the appearance of regions of fast diffusion in the sticky region, where the escape time is relatively short.

In this paper we will answer the following problems. What are the main cantori that surround a given island of stability and how can we approximate them? (sections 2 and 3). How does the size of the island depend on the perturbation, and what is the sequence of the formation of the cantori around it? (sections 4 and 5). How do the various asymptotic curves of unstable orbits, close to a cantorus, cross this cantorus? (section 6). How can we delineate the various secondary sticky regions that surround the main sticky region around an island? (section 7). Finally, our conclusions are summarized in section 8.

2. The sticky regions in a simple model

We study the problem of stickiness in the simple case of the standard map

$$x_{i+1} = x_i + y_{i+1} \qquad (\text{mod } 1)$$
$$y_{i+1} = y_i + \frac{K}{2\pi}\sin(2\pi x_i) \tag{3}$$

where K is the nonlinearity parameter.

When $K = 5$ the phase space is mostly chaotic, but contains two symmetric islands of stability (one of them is shown in figure 1). We consider only every second iteration of the map (3). Thus, the periodic orbit at ($x_c \approx 0.68$, $y_c \approx 0.36$) is considered of period 1. The island surrounding this stable periodic orbit consists of a set of closed invariant curves around the periodic orbit and higher-order islands. The sticky region studied in Contopoulos *et al* (1997) is a thin layer at the outer edge of the island, and further out there is a large chaotic sea. Escape from this sticky region takes place after 10^4–10^9 iterations.

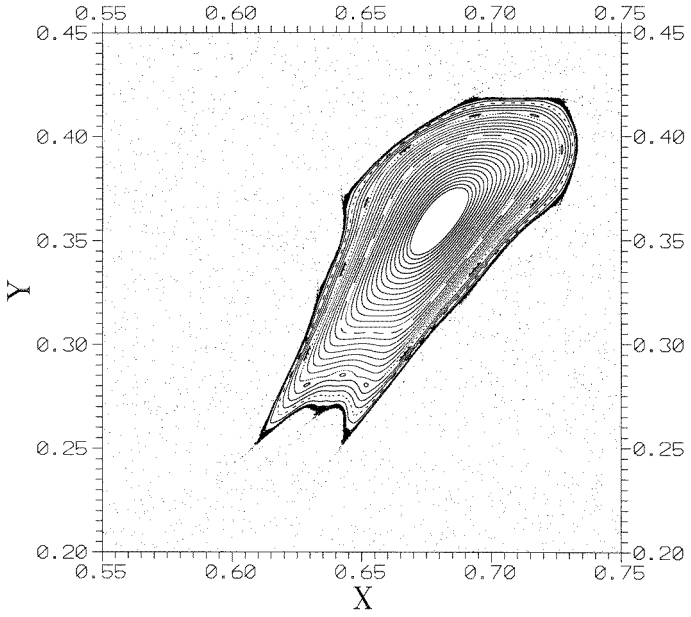

Figure 1. One of the two islands of stability for the standard map with $K = 5$. The narrow dark layer surrounding the island is the main sticky domain. Its boundaries are not well defined and especially the outer boundaries are fuzzy.

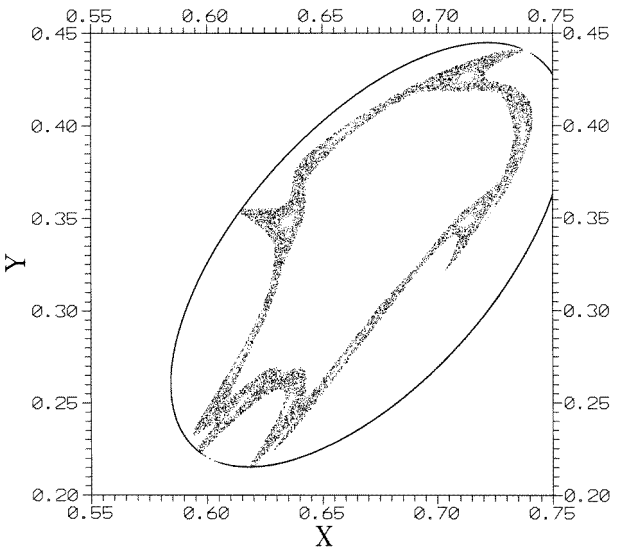

Figure 2. A second sticky region outside the one of figure 1. This contains consequents of a chaotic orbit starting in the large chaotic sea ($x_0 = 0.2$, $y_0 = 0.1$, $K = 5$). Each time the orbit remains for $M > 10$ successive iterations inside the ellipse surrounding the island the last $M - 10$ consequents are plotted.

However, further outside there is a more extended sticky region (figure 2), where stickiness lasts for only 10–10^3 iterations. The points of this sticky region are iterates (Poincaré consequents) belonging to one orbit starting well outside the island, in the chaotic domain. Such iterates are marked in figure 2 only when the orbit (i.e. the set of consequents) stays inside an ellipse surrounding the island for more than 10 iterations. (The ellipse passes roughly through the outermost sticky points of figure 2.) The orbit enters this ellipse at irregular intervals, but most of the time it stays outside it. A comparison of figures 1 and 2 shows that this second sticky region is outside the thin sticky layer of figure 1. Figure 2 shows that *when the orbit stays inside the ellipse* for an extended period then it stays in the dark regions of this figure.

3. Noble numbers and cantori

As mentioned in the introduction the most important cantori are those with noble rotation numbers, i.e. $a = [a_1, a_2, a_3 \ldots]$ when $a_i = 1$ for $i > N + 1$. The number N is called the 'order of the noble number', for example the noble number $[2, 1, 1, \ldots]$ is of first order, while the golden mean $[1, 1, \ldots]$ is of order zero.

The sequence of first-order noble rotation numbers is:

$$[1, 1, \ldots] > [2, 1, \ldots] > [3, 1, \ldots] > \cdots > [\infty, 1 \ldots] = 0.$$

The second-order noble numbers are between the first-order noble numbers, e.g.

$$[1, 1, \ldots] > \tfrac{1}{2} = [2, \infty, 1 \ldots] > \cdots > [2, 3, 1, \ldots] > [2, 2, 1 \ldots] > [2, 1, 1 \ldots].$$

Thus all second-order noble numbers with a first digit of 2 are larger than the corresponding first-order noble number $[2, 1, \ldots]$.

In particular the second-order noble numbers with first digit 1 are larger than the golden number $[1, 1, \ldots]$:

$$1 = [1, \infty, 1\ldots] > \cdots > [1, 3, 1\ldots] > [1, 2, 1\ldots] > [1, 1, \ldots].$$

Similarly, the third-order noble rotation numbers are between the second-order numbers, e.g.

$$[1, 1, 1\ldots] > [1, 1, 2, 1\ldots] > [1, 1, 3, 1\ldots] > \cdots > [1, 1, \infty, 1\ldots] = \tfrac{1}{2}.$$

We note that the increase of the *second* digit of the golden number produces a *larger* number, while the increase of the *third* digit produces a *smaller* number. Similarly the increase of the nth digit produces a *larger* number if n is *even*, and a *smaller* number if n is *odd*.

An important cantorus around the island of figure 1 for $K = 5$ is the cantorus with rotation number $a = [2, 4, 1, 1, \ldots]$. We call this a second-order cantorus. The successive truncations of the noble number $a = [2, 4, 1, 1\ldots]$ are

$$\tfrac{1}{2}, \tfrac{4}{9}, \tfrac{5}{11}, \tfrac{9}{20}, \tfrac{14}{31}, \tfrac{23}{51}, \tfrac{37}{82}, \tfrac{60}{133}, \tfrac{97}{215}, \tfrac{157}{348}, \tfrac{254}{563}, \ldots. \tag{4}$$

Each rational of this sequence has as numerator and denominator the sums of the numerators and denominators of the two previous rationals. In fact the successive truncations of any noble number belong to a Farey tree (figure 3). This tree leads to several neighbouring noble numbers. The sequence leading to the noble number $[2, 4, 1, \ldots]$ is marked by arrows.

For every rational n/m of sequence (4) corresponds at least two periodic orbits. These orbits are generated from the central periodic orbit (of period 1) in pairs (one stable and one unstable) at particular values $K_{n/m}$ of the perturbation (Poincaré 1899, p 213). The stable orbits are surrounded by islands.

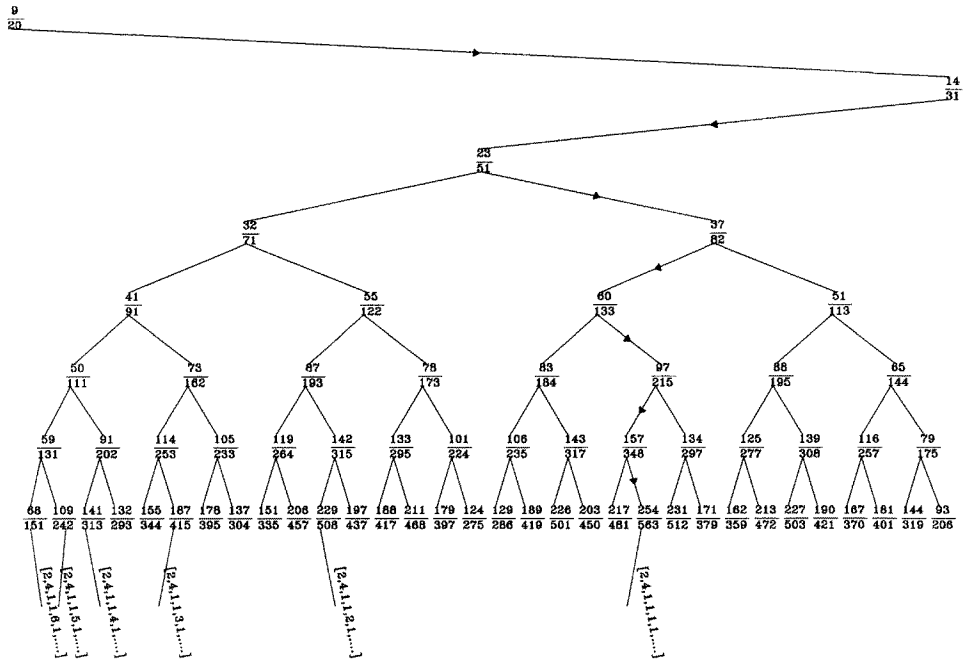

Figure 3. A part of the Farey tree corresponding to the sequence of rational truncations of the noble number $[2, 4, 1, 1, \ldots]$ and of the higher-order noble numbers $[2, 4, 1, 1, q, 1, \ldots]$, $q = 2, \ldots, 6$.

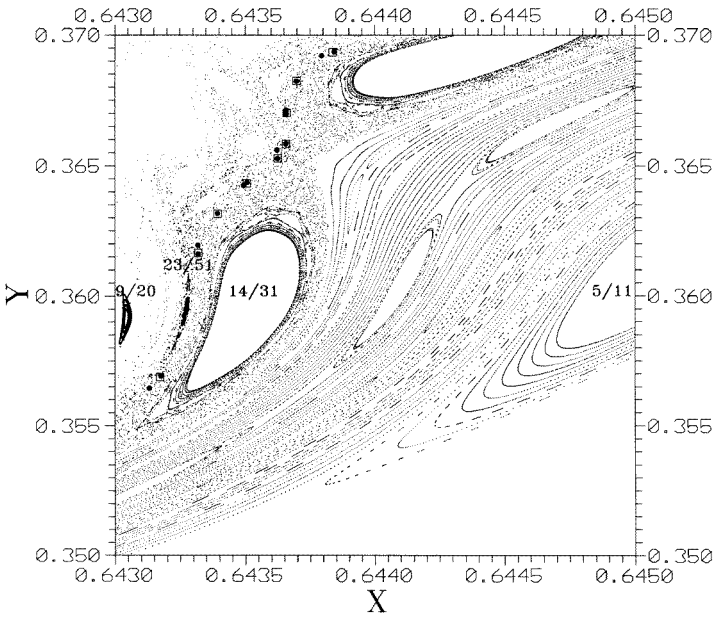

Figure 4. Some islands and periodic orbits around the noble cantorus $a = [2, 4, 1, 1 \ldots]$. Orbits $\frac{97}{215}$ (squares) and $\frac{157}{348}$ (full circles).

As the perturbation K increases, the periodic orbits appear with increasing values of their rotation number. Thus, the orbit $\frac{4}{9}$ is generated at the value $K_{4/9} = 4.8765$, the orbit $\frac{5}{11}$ is generated at the value $K_{5/11} = 4.9117$, and all the orbits of higher order in the sequence (4) after $\frac{5}{11}$ are generated at values of K between $K_{4/9}$ and $K_{5/11}$.

As the order of truncation increases the set of points of the periodic orbit approaches closer and closer the corresponding cantorus. In figure 4 we see some islands from sequence (4). Namely we see the islands $\frac{5}{11}$ and $\frac{14}{31}$ inside the cantorus and the island $\frac{9}{20}$ outside the cantorus. We also see the periodic orbits $\frac{97}{215}$ (squares) inside the cantorus, and $\frac{157}{348}$ (black dots) outside the cantorus. These periodic orbits are very close to the cantorus. For example, most black dots (orbit 348) are inside the squares of the orbit 215 (not at their centres of course). Only four dark dots are slightly outside the line defined by the sequence of squares. As the value of K increases, the stable periodic orbits become unstable generating also new families of periodic orbits. For a value of K larger than the critical value K_c at which a cantorus is formed all the periodic orbits close to the cantorus are unstable.

Figure 5 shows part of figure 4 in greater detail. Namely, we see the islands $\frac{9}{20}$ and $\frac{23}{51}$ outside the cantorus, and $\frac{14}{31}$ inside the cantorus. (The island $\frac{32}{71}$ does not belong to sequence (4).) We mark also the periodic orbit $\frac{254}{563}$ (black squares), which is extremely close to the cantorus.

Figure 6 gives the overall structure of the periodic orbits $\frac{97}{215}$ (white squares) and $\frac{157}{348}$ (black dots). These orbits are in the sticky (black) region of figure 1 and just inside the inner boundary of the outer sticky region of figure 2. In the scale of figure 6 all the dots are inside the squares. Thus, although the orbit $\frac{97}{215}$ is inside the cantorus and the orbit $\frac{157}{348}$ outside it, they are not separated in the scale of this figure. The separation of the periodic orbits corresponding to the various truncations of the noble number is seen in greater detail in figure 7. The periodic orbit $\frac{254}{563}$ is very close to the periodic orbits $\frac{60}{133}$, $\frac{97}{215}$,

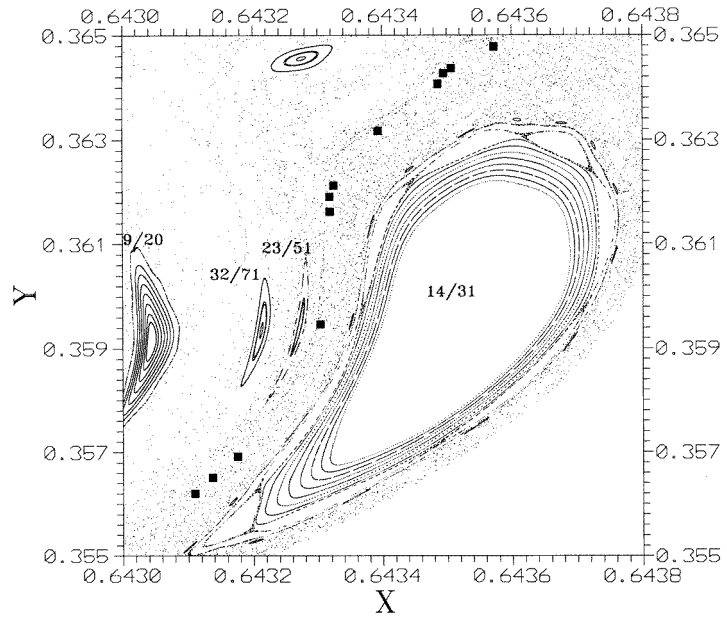

Figure 5. A closer neighbourhood of the cantorus $a = [2, 4, 1, 1, \ldots]$, including points of the periodic orbit $\frac{254}{563}$ (full square).

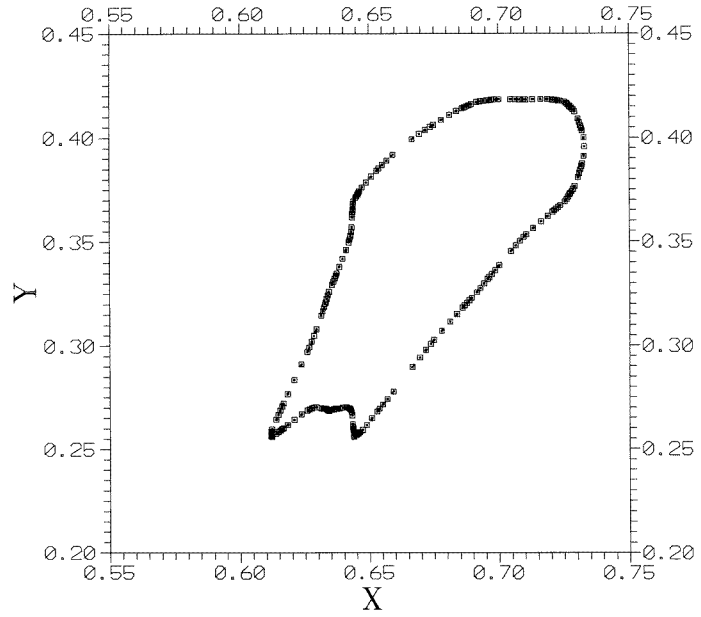

Figure 6. The periodic orbits $\frac{97}{125}$ (empty squares) and $\frac{157}{348}$ (full circles) are very close to the cantorus $a = [2, 4, 1, 1, \ldots]$.

and $\frac{157}{348}$. In particular, the orbits $\frac{60}{133}$ and $\frac{157}{348}$ (outside the cantorus), taken together, define some gaps and the orbit $\frac{254}{563}$ (inside the cantorus) defines essentially the same gaps. (Most prominent are two large gaps above and below the point ($x = 0.6433$, $y = 0.3595$).) Thus

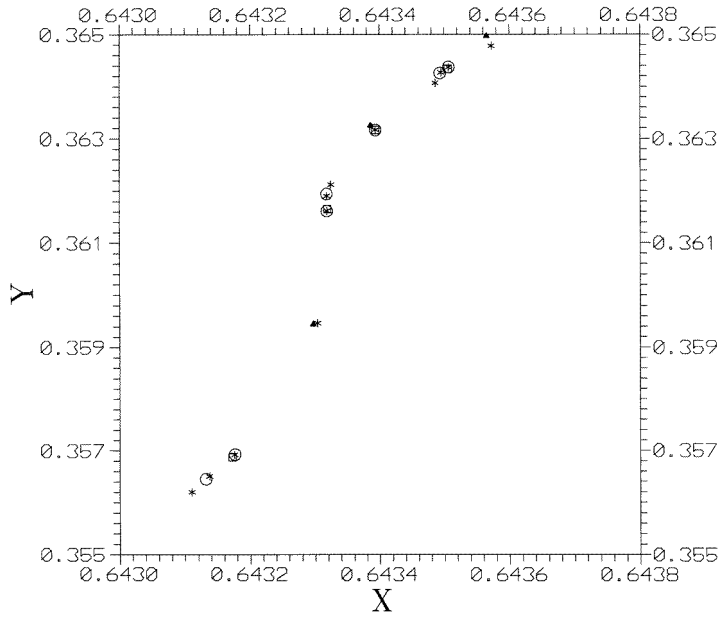

Figure 7. Periodic orbits very close to the cantorus $a = [2, 4, 1, 1, \ldots]$. $\frac{60}{133}$ (triangles) $\frac{97}{215}$ (squares), $\frac{157}{348}$ (circles) and $\frac{254}{563}$ (stars).

there is a tendency of the set of periodic orbits to approach a limit, namely the cantorus $[2, 4, 1, 1, \ldots]$. We stress the fact that in figure 7 no point of the orbit $\frac{254}{563}$ lies in the gaps defined by the lower-order orbits. Thus the gaps seen in figure 7 belong to the cantorus and are not expected to be filled by higher approximations of the cantorus. This fact is important when calculating the lobes of the asymptotic curves that pass through these gaps and produce the observed diffusion through the cantorus (see section 6).

4. Size of the islands

As the nonlinearity K increases, the stable and unstable periodic orbits, generated at the centre of the main island, move outwards. At the same time the KAM curves of given rotation numbers move outwards. But these KAM curves are destroyed and form cantori.

Thus as K increases we have two competing effects that affect the size of the main island. On one hand, the expansion of the tori with given rotation number and on the other hand, the destruction of the outer tori. The size of the island decreases in the long run (for large variation of K), but this decrease is not smooth, and sometimes it is interrupted by a temporary increase of the size of the island.

The decrease is abrupt when a torus, closely surrounding a set of large secondary islands, becomes a cantorus and the large outer chaotic domain joins the region around the islands and separates them from the main island. An example is given in figures 8(a) and (b). In the first case ($K = 4.79$) the five secondary islands $\frac{2}{5}$ are inside a closed torus belonging to the main island. Between the five secondary islands there are five points representing a period-5 unstable periodic orbit, and these points are followed by a chaotic domain, that surrounds all five islands, but does not communicate with the outer large chaotic sea, because of the existence of a separating torus with noble rotation number $[2, 1, \ldots]$. However, for $K = 4.8$

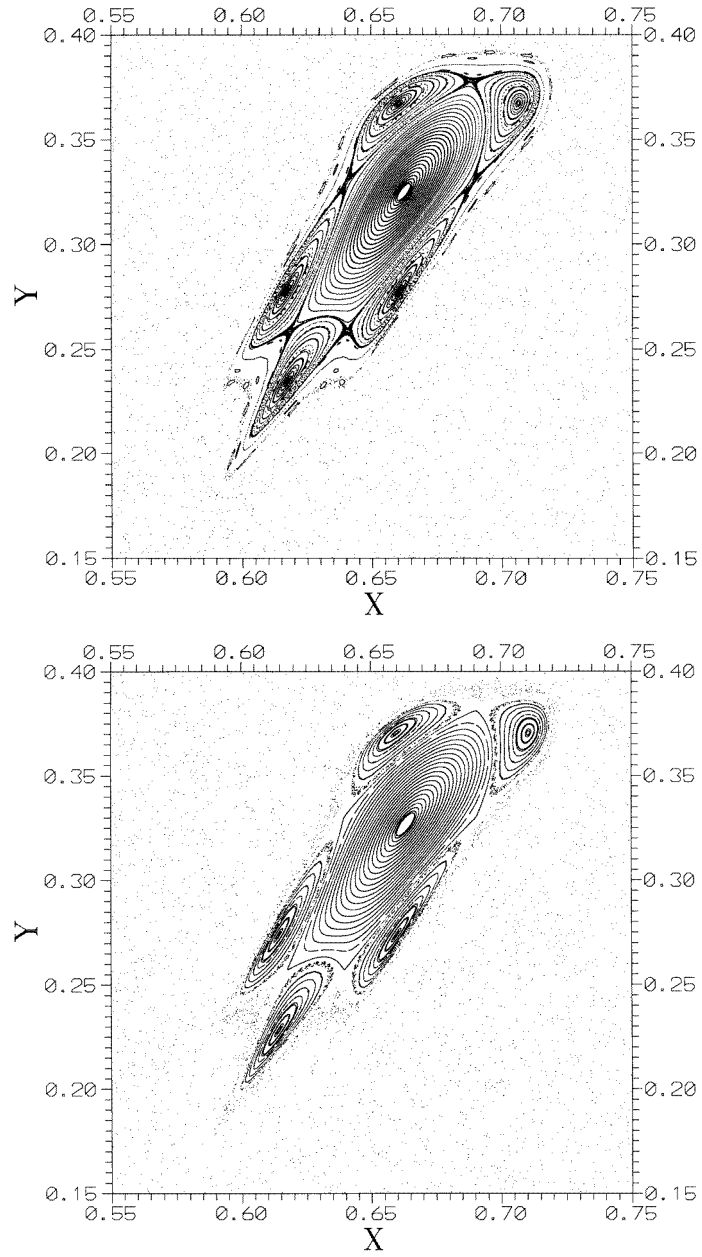

Figure 8. The set of five islands around the main island. This is surrounded by a torus around the centre for (*a*) $K = 4.79$, but it is separated from the main island for (*b*) $K = 4.8$.

this noble torus has been destroyed (it has become a cantorus) and the inner chaotic domain communicates with the outer chaotic sea. As a consequence the size of the main island decreases abruptly by a large jump.

When K increases further, the expansion of the invariant curves dominates over the destruction of the outer invariant curves, and the size of the main island increases. This

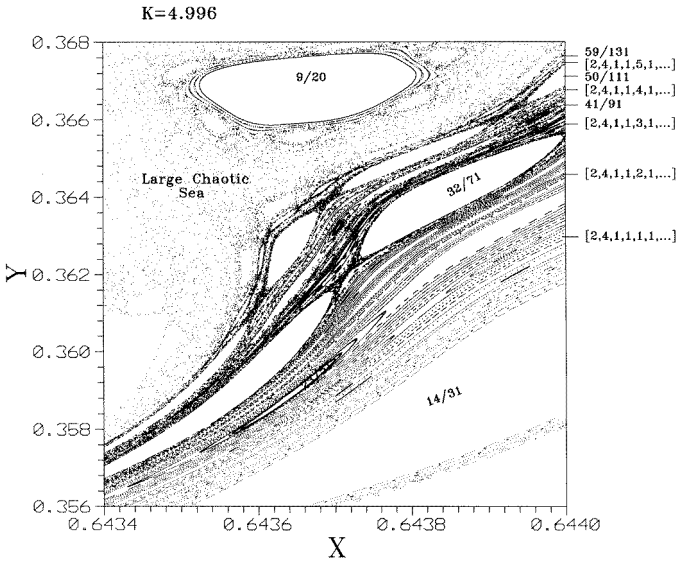

Figure 9. Islands and parts of tori and of the large chaotic sea surrounding the main island, for $K = 4.996$.

can be seen if we compare figure 8(b) (for $K = 4.8$) with figure 1 (for $K = 5$). The main island of figure 1 is larger than the one of figure 8(b).

However, as K increases further, the main island shrinks and for $K = 7$ it has disappeared.

5. Sequence of formation of cantori

The question is now: What is the sequence of the destruction of the various noble curves, and the formation of the corresponding cantori?

In figures 9 and 10 we show a region near the outer boundary of the main island for $K = 4.996$ and $K = 4.997$ respectively.

In figure 9 we see the islands with rotation numbers $\frac{9}{20}$, $\frac{14}{31}$, $\frac{23}{51}$, $\frac{32}{71}$, $\frac{41}{91}$, $\frac{50}{111}$, $\frac{59}{131}$. In between these rational numbers are the noble numbers $[2, 4, 1, 1, q, 1, \ldots]$, $q = 1, 5$ in the sequence:

$$\frac{14}{31} > [2, 4, 1, 1, 1, 1, \ldots] > \frac{23}{51} > [2, 4, 1, 1, 2, 1, \ldots] >$$
$$\frac{32}{71} > [2, 4, 1, 1, 3, 1, \ldots] > \frac{41}{91} > [2, 4, 1, 1, 4, 1, \ldots] >$$
$$\frac{50}{111} > [2, 4, 1, 1, 5, 1, \ldots] > \frac{59}{131}.$$

A careful examination of figure 9 shows that the noble torus $[2, 4, 1, 1, 5, 1 \ldots]$ has been destroyed into a cantorus, but the tori $[2, 4, 1, 1, 4, 1 \ldots]$, $[2, 4, 1, 1, 3, 1 \ldots]$, $[2, 4, 1, 1, 2, 1 \ldots]$ etc, still exist. On the other hand, in figure 10 we see that the tori $[2, 4, 1, 1, 4, 1 \ldots]$, $[2, 4, 1, 1, 3, 1 \ldots]$ have been destroyed, but the tori $[2, 4, 1, 1, 2, 1 \ldots]$, $[2, 4, 1, 1 \ldots]$ etc, still remain.

Thus, as K increases, it seems that the chaotic zone increases only from the outer side inwards, destroying the corresponding noble tori of the sequence $[2, 4, 1, 1, q, 1 \ldots]$ one by one with decreasing q.

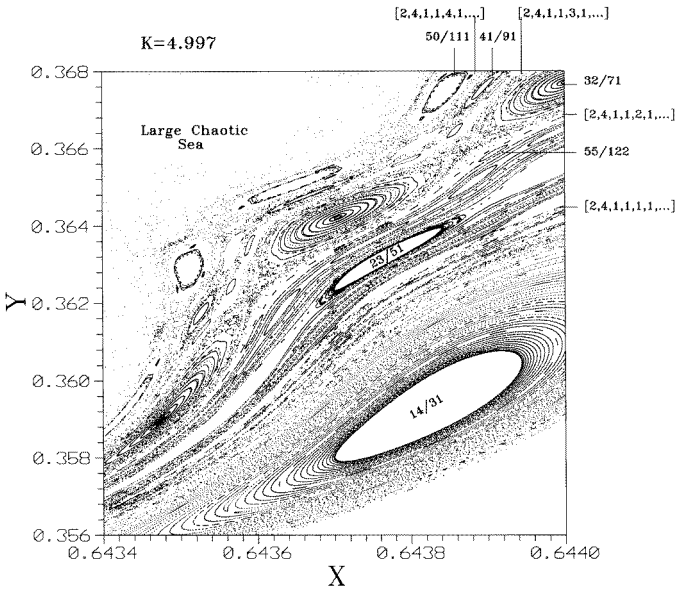

Figure 10. As in figure 9 for $K = 4.997$. The tori with rotation numbers [2, 4, 1, 1, 4, 1, ...] and [2, 4, 1, 1, 3, 1, ...] have been destroyed (have become cantori), but the tori [2, 4, 1, 1, 2, 1, ...] and [2, 4, 1, 1, ...] still exist.

However, it is probable that this consecutive destruction inwards no longer applies for even higher-order noble tori. The reason is as follows. Before the destruction of a certain noble torus, the resonances corresponding to its successive truncations on the inner side contain chaotic zones that destroy higher-order noble tori inside the given torus.

This phenomenon is evident when we have resonant zones with large islands, and large chaotic zones between them, and this happens for relatively low-order noble tori.

Such an example is shown in figures 11 and 12. These figures contain a region near the outer boundary of the main island for values of $K = 4.791$ (figure 11) and $K = 4.793$ (figure 12).

In both cases we see a large inner chaotic layer around the unstable points $\frac{2}{5}$. This layer surrounds the main island and the five islands $\frac{2}{5}$. However, it does not communicate with the outer chaotic sea, lying beyond the region around the noble rotation number [2, 1, ...]. The torus [2, 1, ...] existed for $K = 4.79$ but has been destroyed for $K = 4.791$ and has been transformed into a cantorus. In fact other tori, just inside the cantorus [2, 1, ...], form a boundary layer, still separating the chaotic layer $\frac{2}{5}$ from the large outer chaotic sea. Such tori are [2, 1, 1, 2, 1, ...], [2, 1, 1, 3, 1, ...] and [2, 1, 1, 4, 1, ...] (figure 11).

In figure 11 we see that the torus [2, 1, 1, 5, 1, ...], on the outer boundary of the inner chaotic layer, has been destroyed into a cantorus (for a somewhat smaller value of K). But as we compare figures 11 and 12, we see that the tori of figure 11 [2, 1, 1, 2, 1, ...] on the outer side of the boundary layer and [2, 1, 1, 4, 1, ...] on the inner side of this boundary layer, have been destroyed in figure 12, and only the torus [2, 1, 1, 3, 1 ...] still exists (and some higher-order noble tori also). But for $K = 4.794$ the noble torus [2, 1, 1, 3, 1, ...] has been also destroyed and the chaotic layer close to $\frac{2}{5}$ communicates with the outer chaotic sea.

Thus the destruction of the boundary layer separating the chaotic layer $\frac{2}{5}$ from the outer

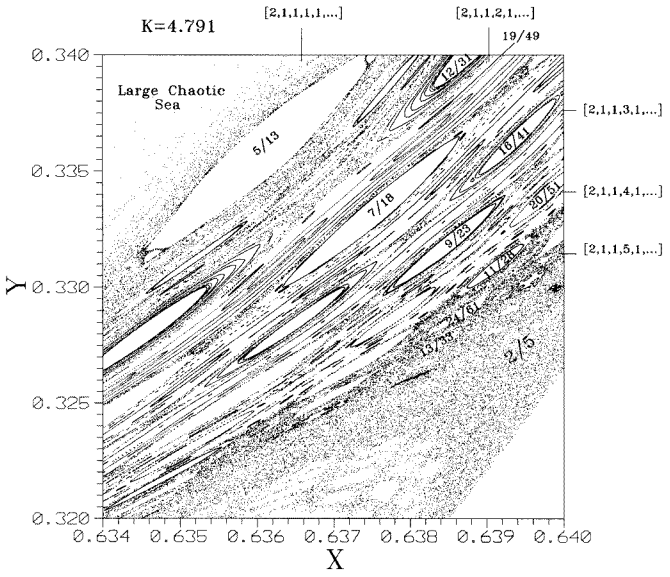

Figure 11. Islands and parts of tori, surrounding the main island for $K = 4.791$. We mark also the large chaotic sea, and a chaotic domain around the unstable orbit $\frac{2}{5}$.

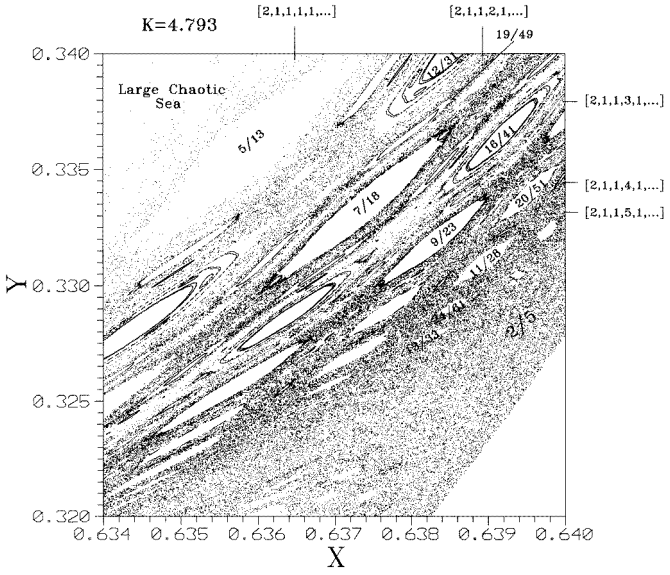

Figure 12. Same as in figure 11 for $K = 4.793$.

chaotic sea proceeds both from outside and from inside. It is obvious that in this case the noble tori $[2, 1, 1, q, 1, \ldots]$ are not destroyed sequentially as q increases from 1 to 5. We have first the destruction of the noble torus with $q = 5$, then those with $q = 1$, $q = 4$ and $q = 3$.

The destruction of tori with even higher values of q has started even before the destruction of the noble torus $[2, 1, 1, \ldots]$ that has $q = 1$.

Thus the increase of the chaotic sea and the eventual destruction of all tori of the main stable island proceeds in steps as follows. For any given K chaotic layers appear near each unstable periodic orbit inside the last KAM curve (the last torus around the centre of the island). As K increases these chaotic layers increase in size. This phenomenon is most conspicuous near the lowest-order resonances, where we have also the largest secondary islands inside the last KAM curve (like the five islands of figure 8(a)). The increase of the size of the chaotic layer is followed by the destruction of tori surrounding the main island (like [2, 1, 1, 5, . . .] of figure 11), and also of tori surrounding the secondary islands (the five islands of figures 8(a) and 11). As K increases further, the tori separating the chaotic layer from the chaotic sea are destroyed, both from the outside and inside. When the last KAM torus in the separating region (e.g. the torus [2, 1, 1, 3, 1, ..] of figure 11) is destroyed, the large chaotic sea communicates with the chaotic layer. Then the last KAM around the main island recedes abruptly to a region inside the chaotic layer (inside the layer $\frac{2}{5}$ in the above case).

This procedure is repeated again and again. After the destruction of the tori surrounding the layer of islands $\frac{2}{5}$ we have the destruction of the tori surrounding the layer around $\frac{3}{7}$ etc.

6. Asymptotic curves and crossing of the cantori

As stated in the introduction, the best way to study the diffusion through a cantorus is by calculating the asymptotic curves that cross the cantorus. In fact the asymptotic curves of unstable periodic orbits form barriers that cannot be crossed by other orbits. Thus, only when the asymptotic orbits themselves cross the cantorus can we have diffusion from one side of the cantorus to the other.

Figure 13 gives, to our knowledge, the first numerical example (non-schematic) of the crossing of a cantorus by an asymptotic curve from the inner to the outer side. The asymptotic curve belongs to the unstable manifold of the unstable periodic orbit $\frac{97}{215}$ (stars) which is inside the cantorus. This is one of the orbits that turned unstable from stable as K increases. The asymptotic curve starts at the point O ($x = 0.643\,319\,077\,512\,8180$, $y = 0.361\,652\,219\,858\,0102$) just above the middle of the figure, downwards. After one oscillation inside the cantorus in the lower left of the figure, the asymptotic curve returns just to the right of the original point and forms a lobe upwards that passes clearly out of the cantorus. Then it returns downwards further to the right of the original point and continues upwards, forming oscillations further outside the cantorus. It returns once again inside the cantorus, but continues upwards outside it.

In order to make sure that the asymptotic curve has crossed the cantorus we mark by squares the periodic orbit $\frac{157}{348}$ which is outside the cantorus. It is clear that in the lower left of figure 13 the asymptotic curve is below the stars and the squares, while in the upper part of the figure most of the lobes are above and to the left of both orbits (stars and squares).

The unstable asymptotic curves of other unstable periodic orbits further inside the cantorus cannot cross the unstable asymptotic curve of the orbit $\frac{97}{215}$. They can cross the cantorus only by remaining inside the lobes of the orbit $\frac{97}{215}$. For example we have calculated the asymptotic curves of the orbit $\frac{14}{31}$ which also crosses the cantorus [2, 4, 1, 1 . . .], like the asymptotic curve $\frac{97}{215}$. However, we need a long time (hundreds of oscillations) until the lobes of the orbit $\frac{14}{31}$ go outside the cantorus.

The best way to find the crossing of the cantorus is by calculating the asymptotic curves of periodic orbits very close to it. The reason is that very close to the cantorus the high-

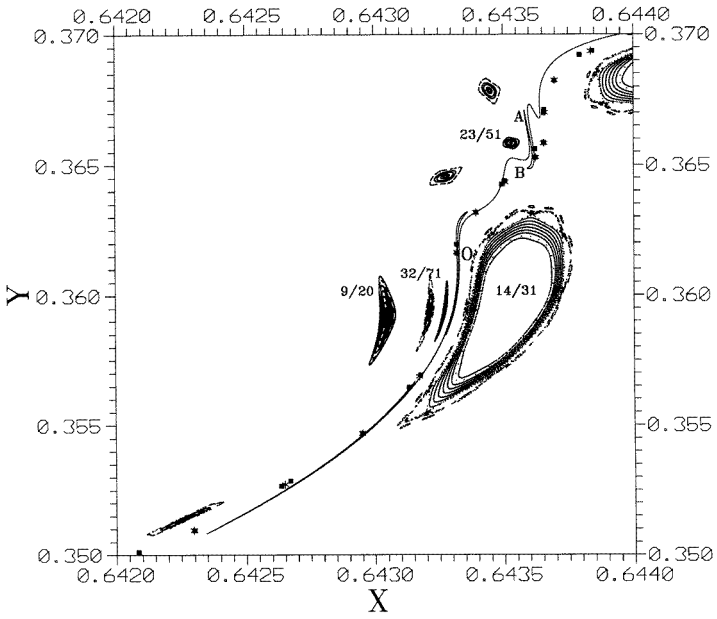

Figure 13. The crossing of the cantorus $[2, 4, 1, 1, \ldots]$ for $K = 5$ by an unstable asymptotic curve of the periodic orbit $\frac{97}{215}$ (stars). The squares belong to the orbit $\frac{157}{348}$. The asymptotic curve starts at the point O downwards, inside the cantorus, but after some oscillations it passes outside the cantorus upwards. Some islands are also marked.

order islands of stability have been destroyed (the stable orbits have become unstable). On the other hand, further away from the cantorus there are still many islands of stability (see figure 13) and the asymptotic curves of periodic orbits even further away must approach the cantorus region by circumventing the various islands, as they cannot cross them.

If we continue the asymptotic curve beyond the loop AB of figure 13, it makes several oscillations back and forth (figure 14) close to the cantorus, crossing it many times inwards and outwards. Only after some more oscillations the asymptotic curve is detached from the cantorus outwards and fills the large chaotic sea. In particular, a part of the line AB in figure 13 after two more iterations gives a curve that makes oscillations far away from the island into the chaotic domain (figure 15).

If the perturbation parameter K is smaller than $K = 4.998$, the cantorus is still a torus and diffusion though it is impossible. All the asymptotic curves of the unstable orbits inside it remain inside forever.

On the other hand, if K is larger, two effects facilitate the diffusion through the cantorus: (a) the gaps of the cantorus become larger, and (b) the islands of stability are destroyed in a larger region around the cantorus. Furthermore, the orbits are much more unstable. As an example we compare the unstable periodic orbit $\frac{97}{215}$ for $K = 5$ and $K = 5.002$. In the first case, the eigenvalue is $\lambda \approx -190$ while in the second case $\lambda \approx -11\,670$. The part of the asymptotic curve shown in figure 13 contains four mappings of the initial segment which is of length 10^{-10}. This length is approximately $10^{-10} \times (190)^4 = 0.13$. On the other hand, the same initial length for $K = 5.002$ is mapped to a total length $10^{-10} \times (11\,760)^4 = 2 \times 10^4$ (figure 16). This length covers the whole phase space 10^4 times. In figures 13 and 16 we have marked the four images of 10^5 points along the initial segment 10^{-10}. In the first case the images are so close to each other that they give the impression of a continuous curve.

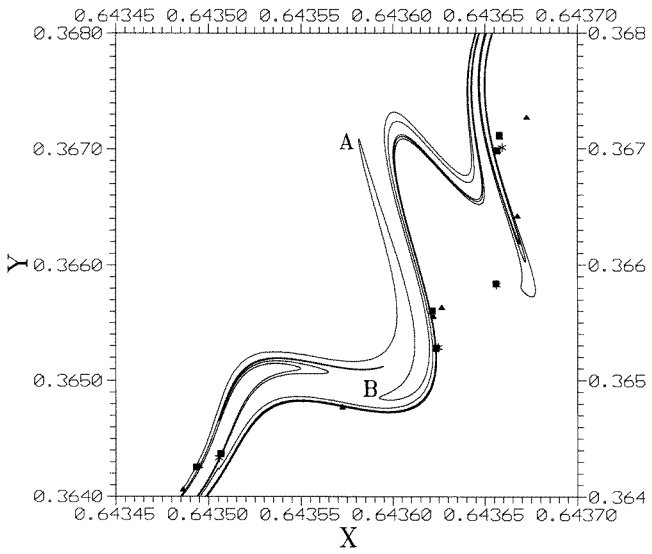

Figure 14. Part of figure 13 in greater detail and for a longer length of the asymptotic curve. The periodic orbits of multiplicities 215, 348 and 563 are marked with stars, squares and triangles respectively. The asymptotic curve passes through *A* and *B* (see figure 13) and then makes several oscillations outside and inside the cantorus (defined approximately by the periodic orbits).

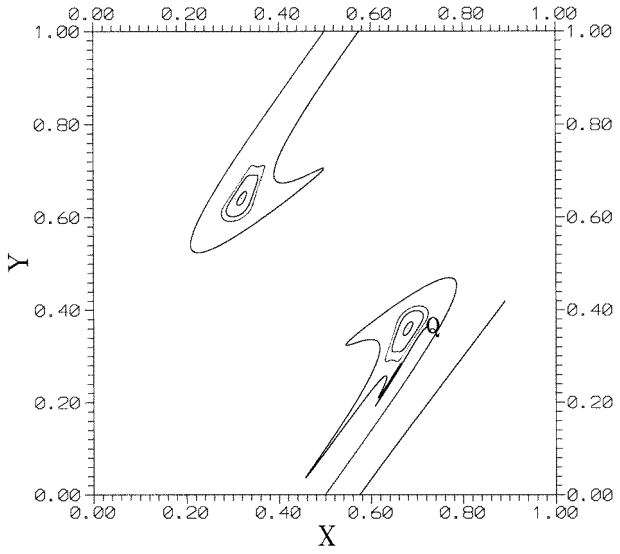

Figure 15. The image of a part of the line AB of figure 13 after two more iterations goes very far from the island into the chaotic domain starting at the point Q. The two main islands are also marked.

However, in the second case the successive points are scattered, because the eigenvalue is so much larger. Only the region close to the right island is dark, due to the effect of stickiness, which is still present in this case. But many points are in the large chaotic sea far from the sticky domain, although the asymptotic curve enters this domain a large number of times.

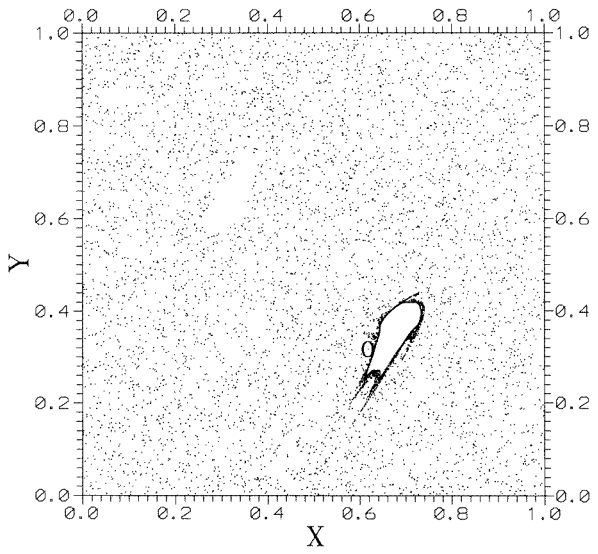

Figure 16. When $K = 5.002$, the points on the asymptotic curve of the orbit $\frac{97}{215}$ as in figure 13 ($K = 5$) are now filling the whole phase space. The initial point is O.

7. Different sticky regions

In our previous paper (Contopoulos *et al* 1997) we described the exponential, or superexponential, dependence of the stickiness (or escape) time on the distance of an initial point of the sticky region from the island of stability. The stickiness time in the main sticky region is usually at least 10^3–10^4 periods, but closer to the island it goes above 10^8. However, further away from the island there are secondary regions where there is some stickiness that lasts 10^2–10^3 periods, and in exceptional cases even longer. In figure 17 we give the stickiness time as a function of x, along the line $y = 0.36$. We see the main sticky region and a heavy curve giving the exponential dependence. If we extrapolate this line to the left it reaches the level 10 iterations at about $x = 0.642$. However on the left of this value we see two features. (a) Extended level lines that correspond to constant low stickiness time of a few times 10, or even less than 10. (b) Regions of relatively high stickiness time, usually between 10^2 and 10^3. If we magnify one such region (figure 18(a), from $x = 0.6322$ to $x = 0.6332$) we see that it separates again into flat regions of constant and relatively low escape time, and regions of high escape time. If we make successive magnifications of one subregion of high escape time of figure 18(a) (figure 18(b), from $x = 0.6331$ to $x = 0.633\,14$, and figure 18(c) from $x = 0.633\,127$ to $x = 0.633\,128$ we see a self-similarity in the separation of regions of high and low escape time. It is thus obvious that the regions of high escape time have a fractal structure.

We have found that the regions of secondary stickiness are defined by the stable manifolds of unstable periodic orbits in the sticky region. In figure 19 we mark the stickiness time as a function of x for various parallel lines of different y, from $y = 0.3505$ to $y = 0.3595$, each separated from the next by $\Delta y = 0.001$. The logarithm of the stickiness time is shown on the right of the figure from 0 to 5 (each level line 5 is 0 for the next value of y). Superimposed in this figure we see the stable asymptotic curves of the unstable periodic orbit $\frac{4}{9}$ which appears in the sticky region a little outside the cantorus $a = [2, 4, 1, 1, \ldots]$. We notice that the lines of the stable manifold separate the regions of

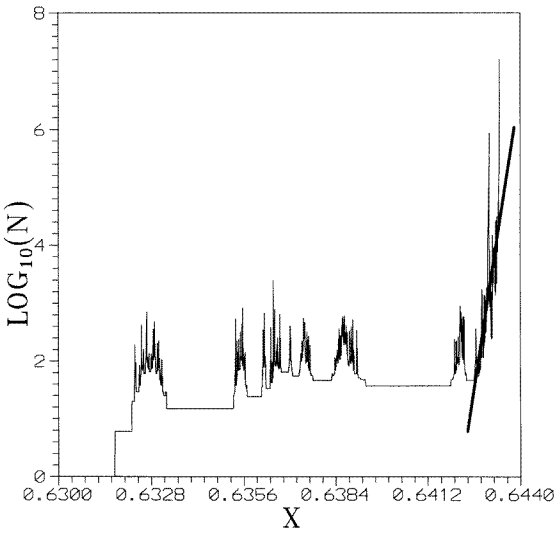

Figure 17. Secondary stickiness regions far from the main island of stability along the line $y = 0.36$. The main sticky region (where the stickiness time reaches 10^8 or more periods) is on the right of $x = 0.642$. The heavy curve in this region represents the exponential dependence of the stickiness time on the distance from the island. But further to the left we see many secondary sticky regions, separated by regions of relative low and almost constant stickiness time.

high and low stickiness time.

The asymptotic curves of figure 19 are extended over a larger part of the phase space in figure 20. We see that the regions of low stickiness time of figure 19 are connected with the large chaotic sea beyond the stickiness domain.

In particular, region A of figure 19 is directly connected with the large chaotic sea at its lower left (figure 20) and escape through this opening is quite fast. Regions B and C of figure 19 also communicate with the large chaotic sea through openings below the lower centre of figure 20 to the left. Similar communications also exist for the other regions of figure 19 that have low and almost constant stickiness time.

In contrast, the orbits in the regions of figure 19 that have relatively high stickiness time (varying widely with x) are trapped in the stickiness domain and escape with difficulty. These orbits do escape from the stickiness domain, but only after a much longer time than the orbits in regions A, B, C etc. Only the orbits that are exactly on the stable asymptotic curves are trapped there forever. However, the measure of these orbits is zero.

The regions of relatively low and high stickiness time are also distinguished by the fact that their spectra of stretching numbers (a) are respectively wide and narrow (Contopoulos and Voglis 1996). This phenomenon will be studied in a future paper.

8. Conclusions

We found the form of the sticky regions around an island of stability, and their relations to the cantori surrounding these regions, and to the asymptotic curves of periodic orbits close to the cantori.

The most important cantori are those with noble rotation numbers. These can be approached closely by higher-order periodic orbits, corresponding to the successive

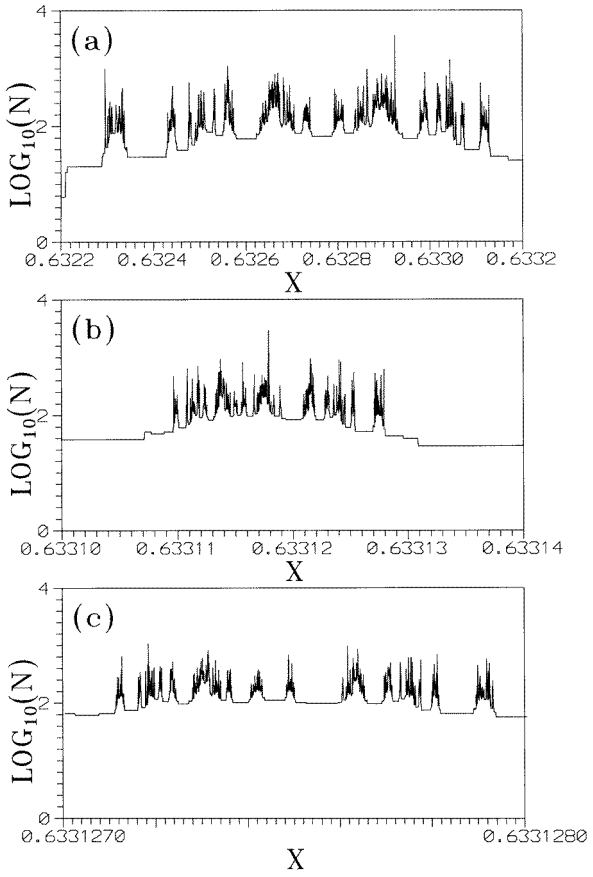

Figure 18. (*a*) One feature of figure 17, seen in greater detail. We see again a structure of local maxima in the stickiness time, separated by regions of low and almost constant stickiness time. (*b*), (*c*) Successive magnifications of one subregion of local maximum of (a).

truncations of the noble numbers.

The main conclusions of our study are as follows.

(1) The size of an island depends on the type and the size of the last KAM curve around it. As the perturbation K increases the size of a given KAM curve (torus) increases. However, at the same time the outer KAM curves are destroyed (they become cantori). Thus, in general the size of an island decreases with K, but it may increase for some intervals of K.

(2) We have found the sequence by which the noble tori are destroyed as K increases in specific cases. In general the destruction proceeds from the outside inwards (towards the centre of the island). However, higher-order noble tori are also destroyed near resonances inside the last KAM curve. Thus the destruction of tori near the last torus proceeds both from outside and inside. As a consequence, when this last KAM torus is destroyed the size of the island decreases abruptly.

(3) The diffusion through cantori can be accurately determined by following the asymptotic curves of nearby unstable periodic orbits. This is a deterministic, non-probabilistic, process.

We give the first (to the best of our knowledge) exact example of the crossing of a

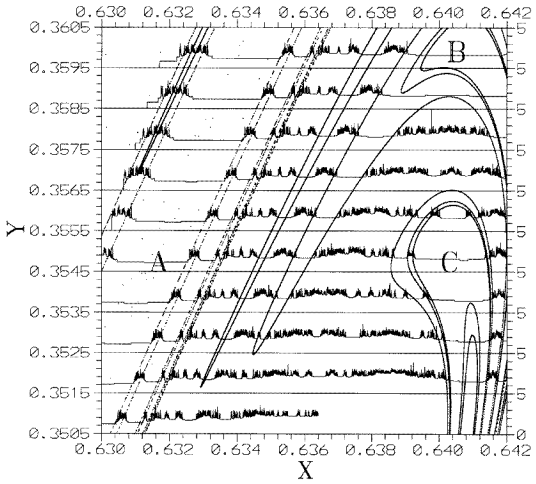

Figure 19. As in figure 17 for various values of y, together with the stable asymptotic curves of the unstable periodic orbit $\frac{4}{9}$.

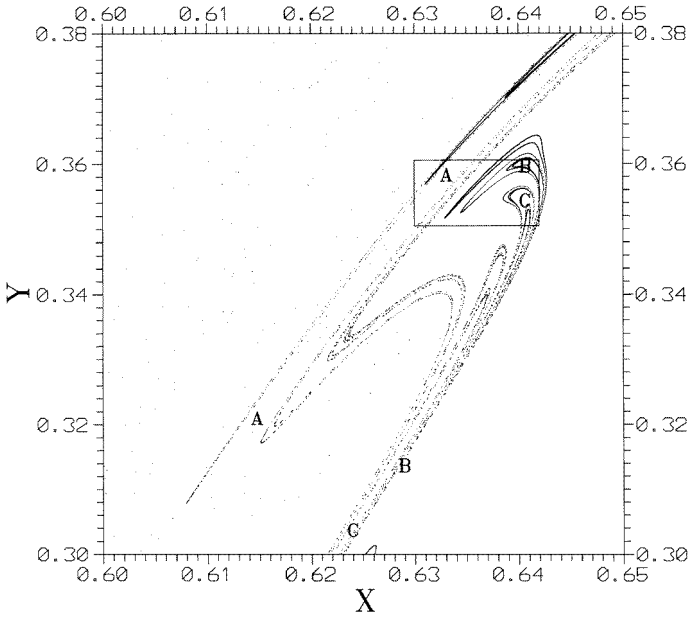

Figure 20. Asymptotic curves of the unstable periodic orbit $\frac{4}{9}$, extending over a larger area than in figure 19 (the area of figure 19 is marked as a parallelogram in this figure). Regions A, B, C communicate with the large chaotic sea.

cantorus by an asymptotic curve of an unstable periodic orbit inside it. The asymptotic curve, after a number of oscillations inside the cantorus, crosses the cantorus several times outwards and inwards, remaining close to the cantorus for a long time. Later the oscillations grow in size and the asymptotic curve goes to large distances.

(4) The asymptotic curves of orbits further inside the cantorus have more difficulties in crossing the cantorus because near the cantorus there is a layer of islands of stability

of higher-order periodic orbits. However, eventually the asymptotic curve approaches the cantorus and crosses it, following closely the asymptotic curves of orbits closer to the cantorus (because these asymptotic curves cannot be crossed).

(5) As the perturbation increases, three effects make diffusion easier: (a) the sizes of the gaps of the cantorus increase; (b) most stable periodic orbits around the cantorus become unstable, and (c) the eigenvalues of the unstable periodic orbits become larger.

Thus, for a modest increase of the perturbation K we have an abrupt increase in the diffusion.

(6) In the main sticky domain around an island, the stickiness time depends exponentially on the distance from the island (and superexponentially very close to the island). But there are more sticky domains where an orbit is trapped for some not very long time. The structure of these secondary sticky domains depends on the forms of the stable asymptotic curves of nearby unstable periodic orbits.

Orbits exactly on the stable asymptotic curves never escape again. But there are also regions close to these stable curves from which escape is relatively slow.

Acknowledgments

We would like to thank a referee for his careful and detailed remarks. This research was supported by the EEC Human Capital and Mobility Program (grant ERB 4050 PL930312) and by the Greek National Secretariat for Research and Technology (PENED 293/1995). CE was supported in part by the Greek Foundation of State Scholarships (IKY).

References

Aubry S 1978 *Solitons and Condensed Matter Physics* ed A R Bishop and T Schneider (Berlin: Springer) p 264
Bensimon D and Kadanoff L P 1984 *Physica* **13D** 82
Contopoulos G 1971 *Astron. J.* **76** 147
Contopoulos G and Voglis N 1996 *Cel. Mech. Dyn. Astron.* **64** 1
Contopoulos G, Varvoglis H and Barbanis B 1987 *Astron. Astrophys.* **172** 55
Contopoulos G, Voglis N, Efthymiopoulos C, Froeschlé C, Gonczi R, Lega E, Dvorak R and Lohinger E 1997 *Cel. Mech. Dyn. Astron.* in press
Greene J M 1979 *J. Math. Phys.* **20** 1183
MacKay R S, Meiss J D and Percival I C 1984 *Physica* **13D** 55
Meiss J D 1992 *Rev. Mod. Phys.* **64** 795
Percival I C 1979 Nonlinear dynamics and the beam-beam interaction ed M Month and J C Herrera (Woodbury, NY: American Institute of Physics) p 302
Poincaré, H 1899 *Les Méthodes Nouvelles de la Mécanique Céleste III* (Paris: Gauthier-Villars)
Shirts R B and Reinhardt W P 1982 *J. Chem. Phys.* **77** 5204